SCIENTIFIC REP🞉RTS

OPEN

Ultrastrong coupling probed by Coherent Population Transfer

G. Falci [1,2,3], A. Ridolfo[1,3,4], P. G. Di Stefano[1] & E. Paladino [1,2,3]

Light-matter interaction, and the understanding of the fundamental physics behind, is the scenario of emerging quantum technologies. Solid state devices allow the exploration of new regimes where ultrastrong coupling strengths are comparable to subsystem energies, and new exotic phenomena like quantum phase transitions and ground-state entanglement occur. While experiments so far provided only spectroscopic evidence of ultrastrong coupling, we propose a new *dynamical* protocol for detecting virtual photon pairs in the dressed eigenstates. This is the fingerprint of the violated conservation of the number of excitations, which heralds the symmetry broken by ultrastrong coupling. We show that in flux-based superconducting architectures this photon production channel can be coherently amplified by Stimulated Raman Adiabatic Passage, providing a *unique* tool for an unambiguous dynamical detection of ultrastrong coupling in present day hardware. This protocol could be a benchmark for control of the dynamics of ultrastrong coupling architectures, in view of applications to quantum information and microwave quantum photonics.

Strong coupling between atoms and quantized modes of an electromagnetic cavity[1] provides a fundamental design building block of architectures for quantum technologies[2]. This regime is achieved when the coupling constant g is large enough to overcome the individual decoherence rates of the mode and of the atom, $g \ll \kappa, \gamma$, and it has been observed in many experimental platforms from standard quantum optical systems[1,3], to architectures of artificial atoms (AA)[4–6]. In such systems small cavity volumes and large AA's dipoles yield values of g up to 1% of the cavity angular frequency ω_c and of the AA excitation energy ε. This allows to perform the rotating wave approximation (RWA) yielding the Jaynes-Cummings (JC) model of quantum optics[1], which describes the dynamics in terms of *individual* excitations exchanged between atom and mode. This process has been largely exploited for quantum control of AA-cavity architectures[5,7,8]. Recently, fabrication techniques have allowed to go beyond, entering the regime of ultrastrong coupling (USC)[9], where $g \sim \omega_c$, ε and the RWA breaks down. So far USC has been detected in superconducting[10–14] and semiconducting[15–18] based architectures essentially via spectroscopic signatures. New physical processes emerge in the USC regime involving multiple photons and many qubits at once[8]. Dynamical detection of population transfer via a USC-specific channel (photon release by decay of the dressed ground state) has been proposed, using spontaneous emission pumping (SEP)[19–21], Raman oscillations[22]. Several dynamical effects have also been predicted, from nonclassical photon statistics[8,23] to Casimir effect[9,24] but despite the large interest, control in time is still an open experimental challenge. Here we show that *coherent* dynamics amplifies fingerprints of USC in *available hardware*. Specifically we prove that a protocol similar to Stimulated Raman Adiabatic Passage (STIRAP) in atomic physics[25–27] operated in the so called Vee (*V*) configuration, provides a unique way to attain coherent population transfer via the USC channel.

Demonstration of coherent dynamics in the USC regime would be a benchmark for quantum control, with appealing applications ranging from microwave quantum technologies[28–32] to dynamical control of quantum phase transitions[33,34].

Results

The quantum Rabi model and STIRAP.
USC between a two-level atom (states $\{|g\rangle, |e\rangle\}$ and energy spitting ε), and a quantized harmonic mode is described by the quantum Rabi model

[1]Dipartimento di Fisica e Astronomia "Ettore Majorana", Università di Catania, Via Santa Sofia 64, 95123, Catania, Italy. [2]CNR-IMM, UOS Università (MATIS), Via Santa Sofia 64, 95123, Catania, Italy. [3]INFN Sezione di Catania, Via Santa Sofia 64, 95123, Catania, Italy. [4]RIKEN, Theoretical Quantum Physics Laboratory, Saitama, 351-0198, Japan. G. Falci, A. Ridolfo, P. G. Di Stefano and E. Paladino contributed equally. Correspondence and requests for materials should be addressed to G.F. (email: gfalci@dmfci.unict.it)
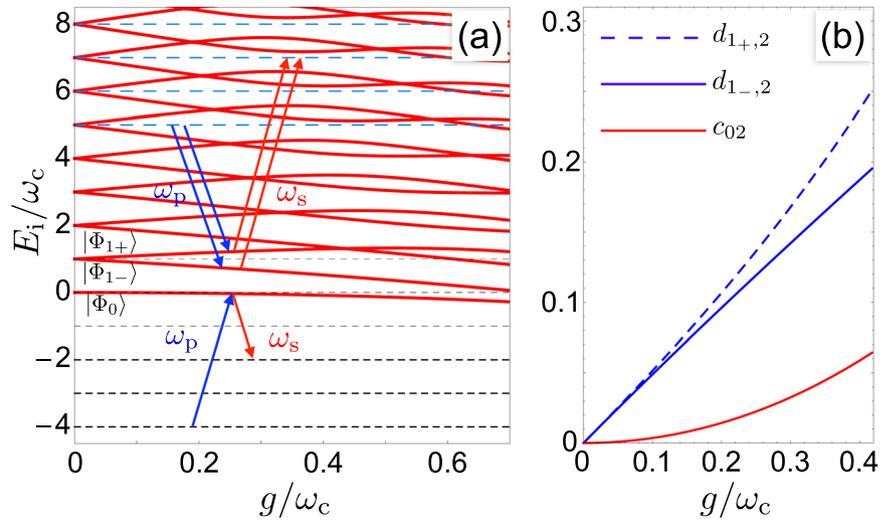
Figure 1. (a) Spectrum of H_R Eq. (1) at resonance (thick red lines): in the JC regime energies are linear in g; deviations yield the Bloch-Siegert shift, marking the onset of USC. Short-dashed black lines are the energies of the low-energy eigenstates $|\nu\rangle$ of the Hamiltonian H_0 ($\varepsilon' = 4\omega_c$) used in the Λ scheme, where two such states are coupled to $|\Phi_0\rangle$ by a pump (ω_p) and a Stokes (ω_s) laser. Long dashed blue lines are energies of states $|\nu\rangle$ used in the V scheme Eq. (9). (b) Amplitudes $c_{02}(g) = \langle 2g|\Phi_0\rangle \propto g^2$ and $d_{1\pm,2} = \langle 2e|\Phi_{1\pm}\rangle \propto g$, relevant for Λ and V-STIRAP, respectively. Here eigenstates $\{|\Phi_0\rangle, |\Phi_{N\pm}\rangle\}$ of the Rabi model for small g/ω_c are labeled by the same quantum numbers of the JC model (See the section Methods).

$$H_R = \varepsilon\,|e\rangle\langle e| + \omega_c\,a^\dagger a + g(a^\dagger|g\rangle\langle e| + a|e\rangle\langle g|)$$
$$+ g(a|g\rangle\langle e| + a^\dagger|e\rangle\langle g|) \tag{1}$$

a ($a^\dagger$) being the annihilation (creation) operators acting on the oscillator Hilbert space spanned by Fock states $|n\rangle$. The RWA can be performed if $g, |\varepsilon - \omega_c| \ll \varepsilon, \omega_c$: the last counterrotating term is neglected yielding the JC Hamiltonian[1] (See the section Methods, whose eigenstates $|\phi_{N\pm}\rangle$ have a defined number N of excitations. In the USC regime $g/\omega_c \sim 0.1 - 1$, the full H_R comes into play, leading to spectroscopic signatures (see Fig. 1(a)) as the Bloch-Siegert shift observed in ref.[11], and drastically altering the JC eigenstates which are mixed by USC. Eigenstates with energy E_j of H_R have the form $|\Phi_j\rangle = \sum_{n=0}^{\infty}[c_{jn}|ng\rangle + d_{jn}|ne\rangle]$, where the only symmetry left implies conservation of the parity of N. In particular the ground state $|\Phi_0\rangle$, which in the JC model is factorized in the zero photon state and the atomic ground state $|0g\rangle$, acquires components with a finite number of photons, corresponding to nonvanishing c_{0n} for n even and d_{0n} for n odd. Proposals of dynamical detection of USC[20,22] aim at the detection of such virtual photons[21] by converting them to real ones. To this end one considers a third ancillary atomic level $|u\rangle$ at a lower energ coupled in the experimentally relevant $-\varepsilon' < 0$[19,20,22,35,36] Assuming that the corresponding transitions are far detuned $\varepsilon' \gg \omega_c$ and $|u\rangle$ is effectively uncoupled, the Hamiltonian becomes (See the section Methods)

$$H_0 = -\varepsilon'|u\rangle\langle u| + H_R + \omega_c\,a^\dagger a \otimes |u\rangle\langle u|. \tag{2}$$

In SEP[26] population is pumped from $|0u\rangle$ to $|\Phi_0\rangle$ and may decay in $|2u\rangle$, due to the finite overlap $c_{02} := \langle 2g|\Phi_0\rangle \neq 0$. The process is forbidden in the JC limit, hence detection of this channel, uniquely leaving two photons in the mode, unveils USC[20]. However SEP would have very low yield, since in most of the present implementations of USC architectures c_{02} is not large enough. This problem is overcome by a striking evolution of SEP, called Λ-STIRAP[25,27], a remarkable technique in atomic physics recently extended to the solid state realm[37–42]. Being based on quantum interference, STIRAP selectively addresses the target state with ~100% efficiency. We now show how this allows to amplify coherently the USC channel. STIRAP is implemented by using a two-tone control field, $W(t) = \sum_{k=p,s} \mathcal{W}_k(t)\cos\omega_k t$, with slowly varying envelopes $\mathcal{W}_k(t)$ driving the AA (See the section Methods). We assume for illustrative purposes that $\varepsilon' \gg \varepsilon$, and choose $\omega_k \sim \varepsilon'$. Thus the field mainly couples to the two lowest atomic states, and the effective control Hamiltonian is given by

$$H_C(t) = W(t)(|u\rangle\langle g| + |g\rangle\langle u|)$$
$$= W(t)\sum_{nj}[c_{jn}|nu\rangle\langle\Phi_j| + c_{jn}^*|\Phi_j\rangle\langle nu|]. \tag{3}$$

By proper choice of the frequencies of the field, $\omega_p \approx E_0 + \varepsilon'$ and $\omega_s \approx E_0 + \varepsilon' - 2\omega_c$, and assuming moreover $\mathcal{W}_k, g \ll \omega_k$, H_C further simplifies yielding the Λ scheme[26] (see Fig. 1(a))
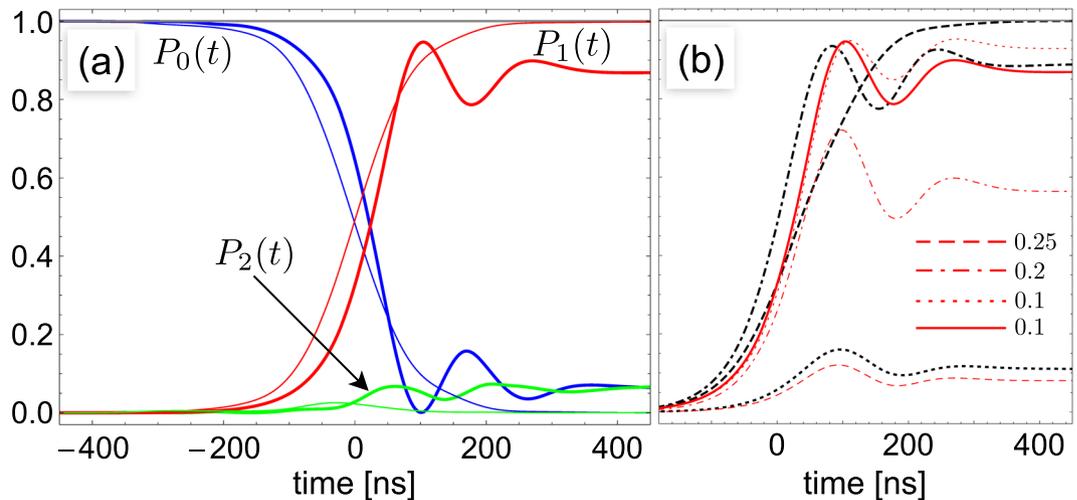
Figure 2. The full Λ-STIRAP dynamics of a AA-harmonic mode system at $\varepsilon = \omega_c$, is studied, using 19 states, $\varepsilon' = 4\varepsilon$ ($\alpha = 3$) and $\Omega_0 T = 900$. Drives are coupled in the experimentally relevant "ladder" configuration $H_C(t) = W(t)[(|u\rangle\langle g| + (1/\eta)|g\rangle\langle e|) + \text{h.c.}]$. Population histories of the three relevant eigenstates $P_0(t) \leftrightarrow |\Psi_{0u}\rangle$, $P_1(t) \leftrightarrow |\Psi_{2u}\rangle$ and $P_2(t) \leftrightarrow |\Psi_0\rangle$ are shown. (**a**) Populations for $g = 0.25$ and $g' = 0$, using Gaussian pulses (thick lines) and crafted pulses compensating Stark shifts (thin lines). (**b**) Population $P_1(t)$ for $g = 0$ and $g' \neq 0$ in the RWA (thick black lines) showing that the JC channel alone may led to population transfer. Red curves refer to $g = 0.25$: for nonvanishing $g'/\omega_c = 0.1, 0.2, 0.25$ (corresponding to $A = 13.3, 6.6, 5.3$) population transfer occurs due to USC only in the first case, the stray channel interfering destructively for larger g'.

$$H_C^\Lambda(t) = \frac{\Omega_p(t)}{2}e^{i\omega_p t}|0\,u\rangle\langle\Phi_0| + \frac{\Omega_s(t)}{2}e^{i\omega_s t}|2\,u\rangle\langle\Phi_0| + \text{h.c.} \tag{4}$$

where $\Omega_p(t) = c_{00}(g)\mathcal{W}_p(t)$ and $\Omega_s(t) = c_{02}(g)\mathcal{W}_s(t)$ are the pump and the Stokes Rabi frequencies, respectively. Under the above assumptions the relevant dynamics involves three levels and it is described by[36]

$$H_3 = -\varepsilon'|0u\rangle\langle 0u| + (2\omega_c - \varepsilon')|2u\rangle\langle 2u| + E_0|\Phi_0\rangle\langle\Phi_0| + H_C^\Lambda(t). \tag{5}$$

The level scheme for Λ-STIRAP is depicted in Fig. 1(a). The problem is conveniently tackled in a doubly rotating frame[25,27] where at double resonance, $\omega_p - \omega_s = 2\omega_c$, the transformed H_3 has an exact instantaneous eigenstate

$$|D\rangle = \frac{\Omega_s(t)}{\sqrt{\Omega_p^2(t) + \Omega_s^2(t)}}|0u\rangle - \frac{\Omega_p(t)}{\sqrt{\Omega_p^2(t) + \Omega_s^2(t)}}|2u\rangle. \tag{6}$$

The system can be trapped in this dark state despite of being excited by the external fields which interfere destructively. If the system is prepared in $|0u\rangle$, Λ-STIRAP[25,27] is obtained by shining two pulses of width T in the "counterintuitive" sequence (the Stokes pulse $\Omega_s(t)$ *before* the pump pulse $\Omega_p(t)$). Then the adiabatic evolution of the dark state yields ~100% population transfer to $|2u\rangle$. Adiabaticity is crucial for this protocol, and it is attained by using large pulse areas $\max_t[\Omega_k(t)]T > 10$ for both fields. Since T is limited by the dephasing time T_ϕ, STIRAP requires appreciable USC mixing $c_{02}(g)$ to yield a large enough Ω_s: if mixing is insufficient population transfer to $|2u\rangle$ does not occur, whereas in the USC regime it occurs with nearly unit probability. Therefore detection of $n = 2$ photons in the cavity at the end of the protocol is a smoking gun for USC.

This simple picture remains valid for the general multilevel dynamics, with driving fields coupled to all the allowed atomic transitions, Fig. 2(a) showing that unit transfer probability is achieved. A key issue is that STIRAP requires g large enough to guarantee adiabaticity for the Stokes pulse, $c_{02}\max_t[\mathcal{W}_s]T > 10$. This (soft) threshold depends *linearly* on $c_{02}(g)$, whereas the efficiency in SEP is much smaller, depending on $|c_{02}(g)|^2$ ($\propto g^4$ for small g, see Fig. 1(b)). Thus *coherence* in STIRAP amplifies population transfer by the USC channel.

Few remarks are in order. We have chosen equal peak Rabi frequencies $\max_t[\Omega_k]$, to ensure robustness against fluctuations, the property making STIRAP successful in atomic physics[26] (See the section Methods), and checked that leakage from the three-level subspace is negligible, as expected since $|\Phi_0\rangle$ is not populated. For small g STIRAP requires a large $\mathcal{W}_s$ (in our simulations its value would yield e–g Rabi oscillations with $\Omega_0 := 600$ MHz) inducing dynamical Stark shifts, and producing a two-photon detuning $\delta(t)$ which may suppress population transfer[27,43]. The problem softens in the multilevel structure, where Stark shifts tend to self-compensate, and may be totally eliminated by using appropriately crafted control[43] (see Fig. 2(a)).

Implementation.   Implementation of the Λ scheme in real devices faces two major problems. Anticipating the central result of our work. we claim that they can be overcome in a unique way by using STIRAP in the Vee (*V*) configuration. The first problem is the reliable detection scheme for the two-photons left in the cavity, which is problematic for THz-photons in semiconductors, while GHz-photons in superconducting AA architectures can be detected with circuit-QED measurement technology[8]. Thus multilevel superconducting AAs offer a natural implementation of our proposal. The second problem is the stray (dispersive) coupling of the mode to AA's transitions involving $|u\rangle$. This has a drastic impact on the reliability of protocols in Λ configuration. We study this point considering an additional stray coupling $g' = \eta g$ between the mode and the AA *u*–*g* transition. For the sake of clarity here we review the main results, postponing details of the analysis to the forthcoming section Effect of stray coupling. We denote with $|\Psi_j\rangle$ the eigenstates of the new Hamiltonian. Insight is gained by perturbation theory in g': due to the stray coupling the intermediate state $|\Phi_0\rangle \to |\Psi_0\rangle$ acquires a component onto $|1u\rangle$ and $|2u\rangle \to |\Psi_{2u}\rangle$ acquires a component onto $|1g\rangle$. Thus the dipole coupling to the Stokes field is modified: keeping only the corotating g' term, to lowest order we find

$$\Omega_s(t) \approx \left[c_{02} - \frac{\sqrt{2}g'^2}{(\varepsilon' - \omega_c)^2 - g^2}\right]\mathcal{W}_s(t).$$

(7)

This shows that g' opens a new channel *already in the RWA*, which allows population transfer to $|\Psi_{2u}\rangle$ even if $c_{02} = 0$. Therefore the final detection of two photons is *not any more* a smoking gun for USC. In general the stray coupling g' interferes destructively with the g-USC channel (see Fig. 2(b)). STIRAP probes *selectively* the USC channel if and only if the correction in Eq. (7) is so small that a large enough pulse width T can be chosen, allowing adiabatic population transfer by the USC channel only. We obtain a necessary condition by treating in perturbation theory also the counterrotating g (details are discussed later)

$$A: = \frac{1}{2\eta^2}\left|\frac{\alpha^2 - (g/\varepsilon)^2}{2 - (g/\varepsilon)^2}\right| \gtrsim 10$$

(8)

where $\alpha := \varepsilon'/\varepsilon - 1$ is the anharmonicity of the AA spectrum. In this regime the two competing contributions to $\Omega_s(t)$ Eq. (7) are both $\propto g^2$, thus the condition Eq. (8) can be severe, and indeed *it is not met by any available design of superconducting AA*. In fact in architectures based on the flux qubit exhibiting the largest figures of USC[10–13], selectivity is lost because the stray coupling is too strong, $\eta \gg 1$. The transmon desing[14], exhibiting the smallest decoherence rates[44,45], offers smaller $\eta \approx 1/\sqrt{2}$, but long coherence times require small anharmonicity, $|\alpha| \lesssim 0.1$, and again selectivity is lost. Figure 2 shows that it is not possible to select the USC channel even with parameters much more favorable than those of state-of the art devices. We remark that for the same reason all previous proposals of dynamical detection[20,22] are ruled out, i.e. present day hardware does not allow to detect unambiguously USC in the Λ scheme.

Vee STIRAP scheme.   The impasse is uniquely overcome by using the *V*-scheme for STIRAP. We consider a flux qubit, the lowest energy doublet being coupled to a harmonic mode in the USC regime[10–13], using the AA's second excited state as the ancillary $|u\rangle$. The system Hamiltonian is

$$H_0 = H_{AA} + H_1 + \omega_c\, a^\dagger a$$

(9)

where $H_{AA} = \varepsilon|e\rangle\langle e| + (2 + \alpha)\varepsilon|u\rangle\langle u|$ describes the flux AA, biased by an external magnetic flux $\Phi_x = \Phi_0/2$, $\Phi_0 = h/2e$ being the flux quantum. This minimizes decoherence[45,46] since H_{AA} is symmetric with respect to fluctuations of Φ_x. The corresponding selection rule forbids *g*–*u* transitions, thus the full coupling to the mode reads

$$H_1 = g\,(a + a^\dagger)[(|g\rangle\langle e| + \eta|e\rangle\langle u|) + \text{h.c.}].$$

(10)

We consider resonant coupling, $\varepsilon = \omega_c$, and a general control field operated via the magnetic flux

$$H_C(t) = W(t)[(|e\rangle\langle u| + (1/\eta)|e\rangle\langle g|) + \text{h.c.}].$$

(11)

We exploit STIRAP via one of the intermediate states $|\Psi_{1\pm}\rangle$, i.e. the two lowest excited states of the Hamiltonian (9) We first neglect the stray coupling *e*–*u* to the mode. Then $|\Psi_{1\pm}\rangle = |\Phi_{1\pm}\rangle$ (see Fig. 1(a)) are eigenstates of H_R, with eigenvalues $E_{1\pm}$, reducing to the JC doublet $(|0e\rangle \pm |1g\rangle)/\sqrt{2}$ when the counterrotating term is switched off. *V*-STIRAP population transfer $|0u\rangle \to |2u\rangle$ is obtained by a two-tone $W(t)$, with $\omega_p = (1 + \alpha)\varepsilon - E_{1\pm}$ and $\omega_s = (3 + \alpha)\varepsilon - E_{1\pm}$. Insight is gained by projecting onto the three-level subspace span$\{|0u\rangle, |2u\rangle, |\Phi_{1\pm}\rangle\}$, yielding an effective Hamiltonian with control

$$H_C^V(t) = \frac{1}{2}[\Omega_p(t)\,e^{-i\omega_p t}|0u\rangle\langle\Phi_{1\pm}| + \Omega_s(t)\,e^{-i\omega_s t}|2u\rangle\langle\Phi_{1\pm}|] + \text{h.c.}$$

(12)

where the Rabi frequencies are now $\Omega_p(t) = d_{1\pm,0}\mathcal{W}_p(t)$ and $\Omega_s(t) = d_{1\pm,2}\mathcal{W}_s(t)$. Since in the absence of counterrotating terms $d_{1\pm,2} = \langle 2e|\Phi_{1\pm}\rangle = 0$ population transfer to $|2u\rangle$ can occur only in the USC regime. Indeed simulations considering the whole multilevel structure (Fig. 3) show that ~100% population transfer efficiency is achieved if and only if the USC regime is attained, *also when the stray coupling is present*. This striking success of *V*-STIRAP, while favored by large anharmonicity ($\alpha \geq 3$) and small ratio between the "ladder" matrix elements
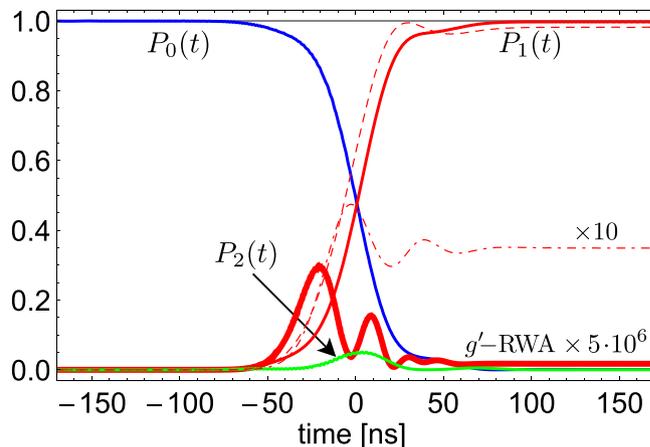
Figure 3. The full V-STIRAP dynamics via the intermediate state $|\Phi_{1-}\rangle \leftrightarrow P_2(t)$ is studied, using 26 states, $\varepsilon' = 2.5\,\varepsilon\,(\alpha = 1.5), \Omega_0 T = 400$. Population histories for $g = 0.25\,\omega_c$ show that transfer to the desired target state occurs both in the absence (thin lines) and in the presence ($P_1(t)$, red dashed line) of a stray coupling $g' = 2/3\,g$. On the contrary no population transfer occurs due to JC couplings: for $g = 0$ and $g' = 0.25\,\omega_c$ in the RWA, $P_1(t) \approx 0$ (red thick line). Instead the counterrotating g'-USC term yields a small residual final population P_1 (red dash dotted line).

($\eta \approx 1/3$) of flux-qubits, has a deeper and robust root: the stray JC coupling g' potentially spoiling USC-selectivity, *is not active in the V-scheme*. Indeed Fig. 3 shows that USC-selective population transfer is attained with parameters $\alpha = 1.5$ and $\eta = 2/3$, not satisfying the requirement Eq. (8), and even worse parameters work. Technical details on the JC channel suppression are given in the next subsection. Here we mention that leading corrections to the control Hamiltonian (12) due to the corotating g' vanish because $\langle nu|\Psi_{1\pm}\rangle = 0$ at lowest order in perturbation theory. This makes V-STIRAP unique as a smoking gun for dynamically probing USC, which again is witnessed by the detection of $n = 2$ photons at the end of the protocol. The probability is approximately the population of $|\Psi_{2u}\rangle$, the stray g' determining only a small probability of detecting a different n ($\sim[\eta\,g/(\alpha\varepsilon)]^2 \sim 10^{-1}(g/\omega_c)^2$, for the simulation in Fig. 3).

The suppression of the JC channel makes V-STIRAP USC-selective also for smaller α, thus lower microwave frequencies can be used for the driving fields, a key experimental advantage. Another asset of V-STIRAP is that since $d_{1\pm2}(g) > c_{0\,2}(g)$ (see Fig. 1(b)) coupling with the Stokes field is larger. Therefore sufficient adiabaticity is attained with smaller T: this minimize decoherence effects and/or softens the problem of stray dynamical Stark shifts since weaker Stokes fields $\mathcal{W}_s$ can be used. Notice indeed that in Fig. 3 shorter time scales than in Fig. 2 were used, and that Stark shifts are not apparent.

Few remarks are in order. We took for granted preparation in the state $|0u\rangle$: for $g = 0$, it is prepared from $|0g\rangle$ by standard pulse sequences[47]. But if $g \neq 0$ the ground state is $|\Phi_0\rangle$ and the above procedure prepares a state which may contain photons. Since the probability $\propto |c_{0n}(g)|^2$ is very small for not so large g, while $d_{1\pm2}(g)$ is large enough to guarantee V-STIRAP population transfer, we expect only some harmless lack of accuracy. Similar arguments ensure that for reasonable parametrization mixing of $|0u\rangle$ due to $g' \neq 0$ is also small. In any case more accurate preparation protocols may be designed to minimize errors.

Concerning decoherence, we know that STIRAP is mainly sensitive to fluctuations in the span{$|0u\rangle$, $|2u\rangle$} subspace and rather insensitive to other processes[45,48]. Efficient population transfer requires $T < T_\phi$, where $1/T_\phi$ is the decoherence rate in the "trapped" subspace, which is approximately the sum of the decay rate κ of the mode and the decay rate $\gamma_{u\to e}$ of $|u\rangle$ in high-quality devices. In such systems these rates are very small, allowing for T up to several dozens of μs. In devices used for USC spectroscopy the mode has a much smaller quality factor, but there should be no fundamental tradeoff between large g and decoherence of the mode alone, allowing for the fabrication of devices exploiting the coherent dynamics in the USC regime. In alternative, with the standard design of high-quality devices large effective couplings $g_{eff} \sim \sqrt{N}g$ could be attained by using few weakly coupled AAs. We checked the dynamics for $N = 4$ AAs, and we reproduced results of Fig. 3 using half of the value of g[49]. We also checked that the protocol is robust against possible inhomogeneities of the individual couplings of AAs and the possible presence of stray additional modes at multiple frequencies.

We stress that for the detection of USC it would be sufficient to monitor the population of the Fock states $|n \geq 2\rangle$ during part of the protocol. Some transient population of the intermediate state is also tolerable, softening the adiabaticity requirement. Decoherence times $T_\phi \sim T$ can also be tolerated[48] since at worst efficiency of the USC-selective channel would be larger than 30%. This opens perspectives also for semiconducting structures, where USC-selective Λ-STIRAP could be observed with some progress in techniques for detecting excess THz photons. We finally mention that a diamagnetic term depending on the specific implementation[50] is included in our Hamiltonian by suitably renormalizing the parameters ω_c and (g, g'). Therefore each setup displaying spetroscopic features of USC will also display the STIRAP dynamics described in this work.
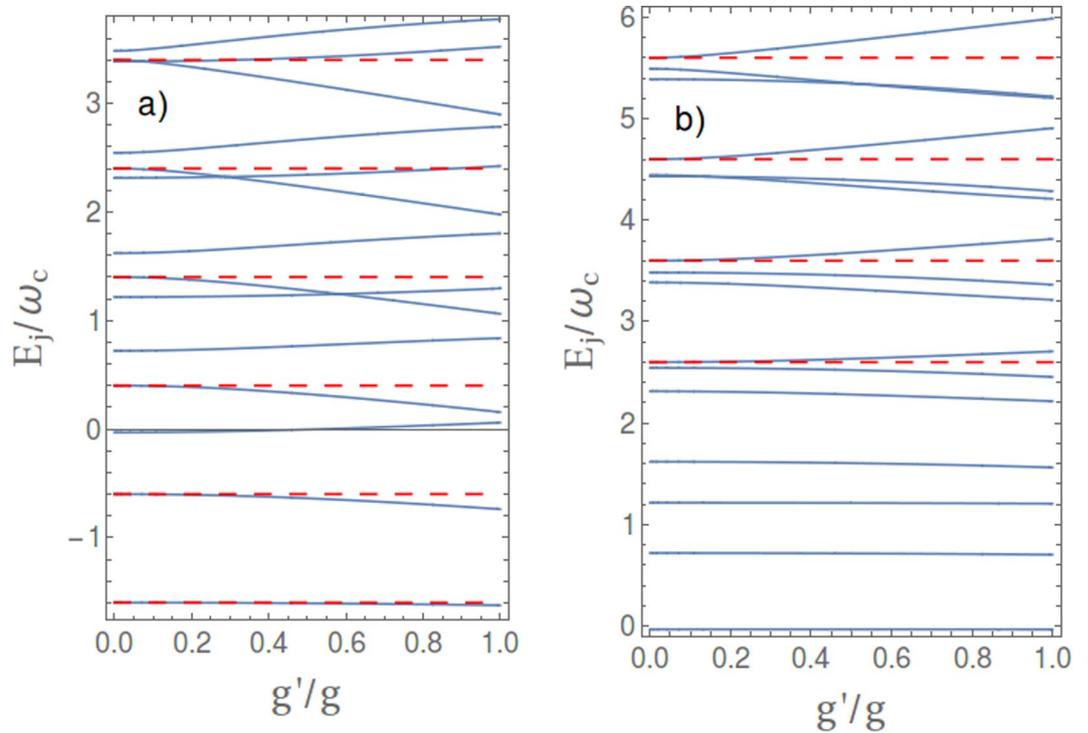
Figure 4. Spectrum of the three-level system coupled in ladder configuration with an harmonic mode, in the USC regime, $g = 0.25\,\omega_c$, with one mode at resonance $\varepsilon = \omega_c$, as a function of the relative strength of the stray coupling $\eta = g'/g$. Red dashed lines are the energies of the uncoupled ancillary states $|nu\rangle$, i.e. when $g' = 0$. (**a**) Spectrum for the level configuration used for the Λ-scheme Eqs (13 and 14), with $\varepsilon_p = 1.6\,\omega_c$. (**b**) Spectrum for the level configuration used for the V-scheme Eqs (20 and 21), with $\varepsilon_p = 1.6\,\omega_c$.

Effect of stray coupling. *Lambda scheme.* We now discuss in more detail the effect of stray couplings. In the Λ scheme we add to the undriven Hamiltonian, Eq. (26), the additional stray coupling $g' = \eta g$ between the mode and the u–g transition, which is the relevant one for AAs. Specifically we consider the more general Hamiltonian $\widetilde{H}_0 = \widetilde{H}_{JC} + \widetilde{H}_c$ where

$$\widetilde{H}_{JC} = -\varepsilon'|u\rangle\langle u| + \varepsilon|e\rangle\langle e| + \omega_c a^\dagger a + [(g\,a|e\rangle\langle g| + g'a|g\rangle\langle u|) + \text{h.c.}] \tag{13}$$

contains all corotating couplings and

$$\widetilde{H}_c = (g_c a^\dagger|e\rangle\langle g| + g'_c a^\dagger|g\rangle\langle u|) + \text{h.c.} \tag{14}$$

are the counterrotating terms. Again $\widetilde{H}_{JC}$ conserves the number N of excitations of the three-level atom plus the harmonic mode, $\hat{N} = a^\dagger a + |g\rangle\langle g| + 2|e\rangle\langle e|$. Eigenstates of $\widetilde{H}_0$, denoted by $|\Psi_j\rangle$, do not possess a well defined N and have the general structure

$$|\Psi_j\rangle = \sum_{n=0}^{\infty} c_{j,n}|ng\rangle + d_{j,n}|ne\rangle + f_{j,n}|nu\rangle \tag{15}$$

where again the parity of N is conserved thus many amplitudes vanish. If the counterrotating $\widetilde{H}_c$ can be treated as a perturbation we can use for $|\Psi_j\rangle$ the same quantum numbers of the JC eigenstates, $j \equiv (N, \tau)$ (see the section Methods), the spectrum being of course different (see Fig. 4a).

To fix the ideas we consider $\omega_c = \varepsilon < \varepsilon'$, and focus on the limit $g' \ll |\varepsilon' - \omega_c|$, hereafter referred as the dispersive regime (for the stray coupling). In this limit it is convenient to classify $|\Psi_j\rangle$ with the same quantum numbers of the JC eigenstates for $g \neq 0$ and $g' = 0$, namely $\{|nu\rangle\} \cup \{|\phi_0\rangle, |\phi_{1\mp}\rangle, \ldots\}$. Focusing on a simple picture where STIRAP involves only levels resonantly coupled by the drives, and letting the two tone pulse couple the intermediate state $|0g\rangle \rightarrow |\Psi_0\rangle$ with $|\Psi_{0u}\rangle$ (pump) and $|\Psi_{2u}\rangle$ (Stokes) the physics is described by an effective three-level Hamiltonian. We now need the matrix elements of the control field in this subspace. To this end we must first diagonalize $\widetilde{H}_0 = \widetilde{H}_{JC} + \widetilde{H}_c$, Eqs (13 and 14). The main structure of the amplitudes is captured by diagonalizing $\widetilde{H}_0$ in the 12–dimensional subspace spanned by the factorized states with $N \leq 4$ excitations. This subspace is enough to account for counterrotating terms in leading (first) order, whereas corotating terms are treated exactly. For the pump field we find

$$\langle\Psi_0|H_C|\Psi_{0u}\rangle \approx W_p(t)\,[c_{0,0}^* f_{0u,0} + f_{0,1}^* c_{0u,1}] \tag{16}$$

The leading term of the matrix element can be found by noticing that all the amplitudes are of order zero in the small quantity $g'_c/(\varepsilon' + \omega_c)$ except $c_{0u,1}$ which is first order, and can be neglected. In particular since in the dispersive regime $f_{0u,0} \approx 1$ the resulting matrix element is $\approx c_{0,0}^* W_p(t)$, i.e. in leading order in the stray coupling the pump matrix element in H_C^Λ is unaffected. Instead for the Stokes field we find substantial differences. The matrix element in the 12–dimensional subspace is

$$\langle\Psi_0|H_C|\Psi_{2u}\rangle \approx W_s(t)[c_{0,2}^* f_{2u,2} + f_{0,1}^* c_{2u,1} + c_{0,0}^* f_{2u,0}] \tag{17}$$

The first term is the Stokes matrix element in H_C^Λ modified by the stray coupling g'. Indeed in the dispersive regime we can approximate $f_{2u,2} \approx 1$, and we recover the expression in H_C^Λ. The two extra terms appearing in Eq. (17) are due to the stray coupling only: the second term is due to the JC part g', whereas the third depends on the counterrotating part and vanishes if $g'_c = 0$.

These extra terms are important since in the physical case $g_c = g$ and $g'_c = g'$ they may be of the same order of the first one, modifying substantially the matrix element. To clarify this point we notice that in the dispersive regime for the stray coupling we also have $c_{0,0}^* \approx 1$ therefore

$$
\begin{aligned}
\langle\Psi_0|H_C(t)|\Psi_{2u}\rangle &\approx W_s(t)\,[c_{0,2}^* + f_{0,1}^* c_{2u,1} + f_{2u,0}]\\
&\approx W_s(t)\left[c_{0,2}^* + c_{2u,1}\left(\frac{g'}{\varepsilon' - \omega_c} + \frac{g'_c}{2\omega_c}\right)\right]
\end{aligned} \tag{18}
$$

where the last line is obtained by estimating extra terms by perturbation theory in g' and g'_c, which gives in leading order

$$
\begin{aligned}
f_{0,1} = \langle 1u|\Psi_0\rangle &\approx \frac{g'}{\varepsilon' - \omega_c}\\
c_{2u,1} = \langle 1g|\Psi_{2u}\rangle &\approx -\sqrt{2}\,g'\frac{\varepsilon' - \omega_c}{(\varepsilon' - \omega_c)^2 - g^2}\\
f_{2u,0} = \langle 0u|\Psi_{2u}\rangle &\approx -\frac{\sqrt{2}\,g'_c g'}{2\omega_c}\frac{\varepsilon' - \omega_c}{(\varepsilon' - \omega_c)^2 - g^2} \approx \frac{g'_c}{2\omega_c}\,c_{2u,1}
\end{aligned} \tag{19}
$$

Notice that our definitions imply that $c_{0,2}^*$ and $c_{2u,1}$ have different signs therefore the extra terms due to stray coupling interfere destructively with the amplitude due to the counterrotating g_c marking USC. In particular this happens even if the stray coupling is purely corotating, i.e. for $g' \neq 0$ and $g'_c = 0$. This remarkable illustrative case corresponds to Eq. (7), showing that a non-vanishing g' yields a nonzero Stokes matrix element even if $g_c = 0$. This is sufficient to determine population transfer to the two-photon target state, if the matrix element the is large enough to guarantee the global adiabaticity condition for STIRAP, $\max_t|\Omega_k(t)|T > 10$. This picture describes also the physics beyond perturbation theory. First of all Fig. 5 shows that the approximation used in this subsection to evaluate the dipole matrix elements are accurate and that the error we make omitting the stray g' corotating term is relevant for the Λ configuration. The consequences for the dynamics are shown in Fig. 2b (black curves) for system of 30 coupled eigenstates, also accounting for the general coupling structure of the two-tone driving field $W(t)$.

The necessary condition for detecting unambiguously the USC channel, Eq. (8) is found by arguing that this latter must satisfy the global adiabaticity condition, $|c_{02}|\mathcal{W}_s T > 10$, while the stray channel does not $|f_{0,1}^* c_{2u,1}|\mathcal{W}_s T < 10$. This determines the weaker criterion $|c_{02}|/|f_{0,1}^* c_{2u,1}| \gg 10$. Equation (8) is obtained by using the perturbative result (25) for $c_{0,2}$, and letting $g_c = g$. Destructive interference of the $g_c = g$ and the g' channels is illustrated in Fig. 2b (red curves), where it is seen that this physical picture holds beyond perturbation theory.

Vee scheme. For STIRAP in the Vee configuration the ancillary atomic level $|u\rangle$ has higher energy. Again we start from a more general Hamiltonian $\widetilde{H}_0 = \widetilde{H}_{JC} + \widetilde{H}_c$ where

$$
\begin{aligned}
\widetilde{H}_{JC} = \ &\varepsilon|e\rangle\langle e| + (\varepsilon + \varepsilon')|u\rangle\langle u| + \omega_c a^\dagger a\\
&+ [(g\,a|e\rangle\langle g| + g'a|u\rangle\langle e|) + \text{h.c.}]
\end{aligned} \tag{20}
$$

contains all corotating couplings, the counterrotating terms being

$$\widetilde{H}_c = (g_c a^\dagger|e\rangle\langle g| + g'_c a^\dagger|u\rangle\langle e|) + \text{h.c.} \tag{21}$$

Eigenstates of $\widetilde{H}_{JC}$ have a well defined number of excitations, $N = a^\dagger a + |e\rangle\langle e| + 2|u\rangle\langle u|$. They are the isolated ground state $|\Phi_0\rangle = |0g\rangle$, a single excitation g-JC doublet $|\Phi_{1\mp}\rangle = |\phi_{1\mp}\rangle$, and $N \geq 2$ triplets $|\Phi_{N\tau}\rangle$ as before. We are interested to the dispersive regime for the stray coupling $g' \ll \varepsilon' - \omega_c$. As for Λ-STIRAP eigenstates are conveniently enumerated by the quantum numbers $\{0u, 1u, \ldots, 0, 1\mp, 2\mp, \ldots\}$, but the energy spectrum is different (see Fig. 4b).
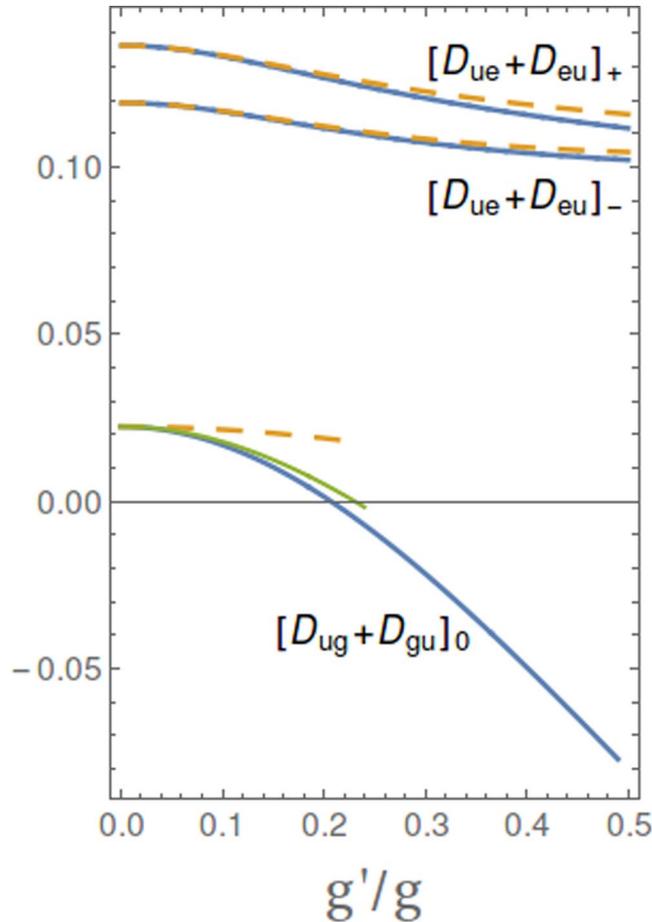
Figure 5. "Dipole" matrix elements for the Stokes field when the three-level system is coupled in ladder configuration with an harmonic mode, in the USC regime, $g = 0.25\,\omega_c$, with one mode at resonance $\varepsilon = \omega_c$, as a function of the relative strength of the stray coupling $\eta = g'/g$. Here $[D_{ug} + D_{gu}]_0 = \langle\Psi_{2u}|[|u\rangle\langle g| + |g\rangle\langle u|]|\Psi_0\rangle$ is relevant for Λ-STIRAP. The full thick line is obtained by diagonalizing a large system, and it is identical to the result of the diagonalization in the 12-dimensional subspace containing $N \leq 4$ excitations (not shown). The full thin line is the approximation we start with to derive Eqs (7 and 8), and includes only the g' corotating interaction. The dashed line is obtained neglecting leading corrections in g'. These results quantitatively illustrate the scenario on the failure of Λ-STIRAP. Instead the behavior of $[D_{ue} + D_{eu}]_{\pm} = \langle\Psi_{2u}|[|u\rangle\langle e| + |e\rangle\langle u|]|\Psi_{1\pm}\rangle$, which enters V-STIRAP, is weakly dependent on g', except for the wavefunction renormalization: the result obtained by diagonalizing a large system (full thick line) is identical to the result of the diagonalization in the subspace containing $N \leq 6$ excitations (not shown), where terms due to the corotating g' are absent. Moreover leading corrections in the counterrotating g' are small.

Eigenstates of $\widetilde{H}_0$ have the same structure Eq. (15), the counterrotating terms mixing subspaces with the same parity of N. Following the same steps of the analysis of Λ-STIRAP we focus on the part of the control term $H_C(t) = W(t)[|u\rangle\langle e| + |e\rangle\langle u|]$ resonant with the $|\Psi_{0u}\rangle \leftrightarrow |\Psi_{1\pm}\rangle$ (pump) and the $|\Psi_{2u}\rangle \leftrightarrow |\Psi_{1\pm}\rangle$ transitions calculating matrix elements by diagonalization of $\widetilde{H}_0$ in the 18–dimensional subspace spanned by states with up to $N \leq 6$ excitations. For the pump field we find

$$\langle\Psi_{1\pm}|H_C|\Psi_{0u}\rangle \approx W_p(t)[d^*_{1\pm,0}f_{0u,0} + f^*_{1\pm,1}d_{0u,1}] \tag{22}$$

which in leading order in g_c and g'_c and in the dispersive regime reduces to $\approx W_p(t)d^*_{1\pm,0}$. Therefore at this level of accuracy the stray coupling does not modify the pump matrix element in H_C^V Eq. (12). For the Stokes field, in leading order in g_c and g'_c, we find

$$\langle\Psi_{1\pm}|H_C|\Psi_{2u}\rangle \approx W_s(t)[d^*_{1\pm,2}f_{2u,2} + d^*_{1\pm,0}f_{2u,0}] \tag{23}$$

Here $d^*_{1\pm,2}$ and $f_{2u,0}$ are first order in the small counterrotating couplings g_c and g'_c whereas in the dispersive regime $f_{2u,2}$, $d^*_{1\pm,0} \to 1$. The remarkable fact is that the matrix element vanishes for both g_c, $g'_c \to 0$, therefore to this level of accuracy no population transfer may occur due to the corotating stray coupling g'. This picture describes also the physics beyond perturbation theory. Figure 5 shows that the the stray g' corotating term does not contribute in a relevant way to the dipole matrix elements entering the Vee configuration. The dynamics

illustrated in Fig. 3, where the whole structure of the drive is accounted for, shows that stray population transfer due to the corotating g' is suppressed by six orders of magnitude even at an accuracy level beyond perturbation theory. Extra contribution is possibly due to the stray counterrotating g'_c, which in the physical situation of Fig. 3 is also very small. Summing up corotating couplings do not produce population transfer, whose observation marks unambiguously the emergence of USC.

Discussion

In conclusion, we propose the dynamical detection of the USC regime of light-matter interaction using an ancillary atomic level as a probe. The opening of a USC-specific channel for population transfer is witnessed by detecting two-photons in the harmonic mode. This process, coherently amplified by STIRAP, marks the symmetry broken by the USC counterrotating g term in H_R Eq. (1), which determines the violation of the conservation of N Relying on coherent dynamics, the experiment we propose would be a benchmark for adiabatic quantum control of circuit QED architectures[36,51] in the USC regime. STIRAP is known to be superior to other protocols[25–27] in the Λ scheme, as SEP[20] or Raman oscillations[22]. What makes it unique is the possibility to operate in V-configuration, which is resilient to the presence of stray AA-mode couplings, inevitable in three-level USC solid state architectures. Flux qubits, offering the largest $g/\omega_c > 1$ fabricated so far, also meet all the quantum hardware requirements for the experiment.

Methods

The Jaynes-Cummings and the Rabi models.   The JC Hamiltonian describes a two-level atom coupled to an electromagnetic mode in the RWA

$$H_{JC} = \varepsilon |e\rangle\langle e| + \omega_c\, a^\dagger a + g\,[a|e\rangle\langle g| + a^\dagger|g\rangle\langle e|] \tag{24}$$

where with no loss of generality we assume $g > 0$. The ground state is factorized $|\phi_0\rangle = |0g\rangle$ with $\mathcal{E}_0 = 0$ whereas the rest of the spectrum is arranged in doublets, $|\phi_{N\sigma}\rangle$, with fixed number of excitations $N = a^\dagger a + |e\rangle\langle e|$ and labeled by the extra quantum number $\sigma = \pm$. At resonance, $\varepsilon = \omega_c$, eigenstates/eigenvalues of H_{JC} in the atom-mode product basis are given by

$$|\phi_{N\mp}\rangle = \frac{|N-1,\,e\rangle \mp |N,\,g\rangle}{\sqrt{2}};\ \ \mathcal{E}_{N\mp} = N\omega_c \mp \sqrt{N}\,g$$

Eigenstates of H_R, Eq. (1) in the main text, do not have a well defined N only its the parity $\sum_n (-1)^n |n\rangle\langle n|\,[|g\rangle\langle g| - |e\rangle\langle e|]$ being conserved. Many of the amplitudes in the decomposition in product states (reported in the text) vanish. For instance for the dressed ground state $|0g\rangle \to |\Phi_0\rangle$ all $c_{0n} := \langle ng|\Phi_0\rangle\,(d_{0\,n} := \langle n\,e|\Phi_0\rangle)$ with odd (even) number of photons n vanish

$$|\Phi_0\rangle = \sum_{m=0}^{\infty}[c_{0\,2m}|2mg\rangle + d_{0\,2m+1}|2m+1\,e\rangle]$$

For not too large g eigenstates $|\Phi_j\rangle$ of the H_R, Eq. (1) in the main text, can be enumerated with the same quantum numbers of the JC limit, $j \equiv (N, \mp)$. For them conservation of the parity of N implies the following structure

$$|\Phi_{N\mp}\rangle = \sum_{m>-N/2}[c_{N\mp,\,N+2m}|N+2m,\ g\rangle + d_{N\mp,N+2m-1}|N+2m-1,\,e\rangle]$$

Some of the essential features of STIRAP in the USC regime emerge already treating the counterrotating term of H_R, Eq. (1) in the main text, in perturbation theory. To this end it is convenient to generalize slightly H_R, Eq. (1) in the main text, by allowing for a different coupling constant $g_c \neq g$ for the counterrotating term. The leading corrections of interest to the JC ground state $|0g\rangle$ are

$$\begin{aligned}
c_{00} &= \langle 0g|\Phi_0\rangle = \frac{4\omega_c^2 - 2g^2}{\sqrt{(4\omega_c^2 - 2g^2)^2 + g_c^2(4\omega_c^2 + 2g^2)}}\\
c_{02} &= \langle 2g|\Phi_0\rangle = g_c\frac{\sqrt{2}\,g}{4\omega_c^2 - 2g^2}
\end{aligned} \tag{25}$$

Notice that these expressions are perturbative in g_c but nonperturbative in g, the JC model being recovered for $g_c \to 0$. The nonzero overlap with the $N > 0$ states marks the emergence of USC. At leading order $c_{02} \propto g_c g$ therefore in the physical case $g_c = g$ the amplitude $c_{02} \propto g^2$ (see Fig. 1(b) in the main text). The fact that STIRAP depends on $\Omega_s \propto |c_{02}|$ while SEP depends on $|c_{02}|^2 \propto g^4$, which is much smaller, is one of the assets of coherent amplification.

The first JC doublet $|\phi_{1\mp}\rangle \to |\Phi_{1\mp}\rangle$ enters V-STIRAP. In this case $\langle 0e|\Phi_{1\mp}\rangle \approx 1/\sqrt{2} \approx \mp\langle 1g|\Phi_{1\mp}\rangle$ the relevant corrections in leading order being

$$d_{1\mp,2} = \langle 2e|\Phi_{1\mp}\rangle = -g_c \frac{2\omega_c \pm g}{(2\omega_c \pm g)^2 - 3g^2}$$

The nonzero overlap of $|\Phi_{1\mp}\rangle$ with the $N > 1$ states marks the emergence of USC. It is worth stressing that the efficiency of V-STIRAP depends on $\Omega_s \propto |c_{1\pm,2}| \propto g_c$, i.e. for relatively small g is much more efficient than Λ–STIRAP.

Lambda STIRAP in the USC regime.   In the simplest instance Λ-STIRAP is obtained by adding an uncoupled atomic level $|u\rangle$ to H_R. In the main text we introduced the resulting Hamiltonian

$$H_0 = -\varepsilon'|u\rangle\langle u| + H_R + \omega_c a^\dagger a \otimes |u\rangle\langle u|. \tag{26}$$

where the last term completes the identity operator for the AA in passing from the two-level system in H_R to the three-level system in H_0. We take $\varepsilon' \gg \varepsilon = \omega_c \gtrsim g, g_c$. The control field is coupled to the AA, and we consider a two tone $W(t)$ with frequencies $\omega_p = E_0 + \varepsilon' + \delta_p$ and $\omega_s = E_0 + \varepsilon' - 2\omega_c + \delta_s$, and for simplicity $\delta_p = \delta_s = 0$ in most simulations. For large ε' the drive couples only with the u–g transition, yielding Eq. (3) in the main text. If g is not too large we can neglect terms with $n > 2$, which are detuned and have smaller amplitude $c_{0n}(g)$. The simple Λ configuration[26] $H_C^\Lambda(t)$ is obtained by retaining the resonant and corotating parts of $W(t)$. In order to operate STIRAP we take slowly varying envelopes with Gaussian shape

$$\mathcal{W}_s(t) = \overline{\mathcal{W}_s}e^{-[(t+\tau)/T]^2}; \;\; \mathcal{W}_p(t) = \overline{\mathcal{W}_p}e^{-[(t-\tau)/T]^2}$$

where the delay $\tau > 0$ implements the "counterintuitive" sequence.

General properties and optimization.   STIRAP relies on resonant external fields inducing destructive interference[25,27]. Faithful and selective coherent population transfer is achieved by adiabatic dynamics[25,27]. Adiabaticity requires sufficiently large pulse amplitudes, satisfying the so called "global condition"[26]

$$c_{00}\overline{\mathcal{W}_p}, c_{02}\overline{\mathcal{W}_s} > 10\,T$$

Besides the efficiency the virtue of STIRAP is the remarkable robustness against variation of the parameters. Indeed STIRAP is not very sensitive to slight deviations from optimal values of the parameters (pulse shapes and amplitudes, detunings and delay), thus efficient amplification of the $|0u\rangle \rightarrow |2u\rangle$ channel does not require fine tuning of too many parameters. In the simulations we used the standard figures $\tau = 0.75\,T$ and $\delta_s = \delta_p = 0$ for conventional STIRAP and since it is known that the best robustness is obtained for equal peak Rabi frequencies[26], $\max_t[\Omega_s(t)] = \max_t[\Omega_p(t)]$, we considered an attenuated pump field

$$\overline{\mathcal{W}_p} = \kappa_p^\Lambda \overline{\mathcal{W}_s}, \;\; \kappa_p^\Lambda = c_{02}(g)/c_{00}(g)$$

In this situation the only relevant sensitivity to take care of is related to deviations from the two-photon resonance condition $\delta = 0$, where $\delta := \delta_s - \delta_p = 2\omega_c - (\omega_p - \omega_s)$ is the two-photon detuning. For $\delta \neq 0$ no exact dark state exists and no adiabatic pattern connects the initial and the target state, but if $|\delta| \lesssim \max_t[\Omega_k(t)]/5$ efficient population transfer still occurs via diabatic processes[26]. These considerations apply to both Λ and V STIRAP.

Dynamical Stark shift compensation.   The simple standard form of the control Hamiltonian in Λ configuration, $H_C^\Lambda(t)$, reported in the text is obtained assuming that field amplitudes $\mathcal{W}_k$ are small enough to be negligible except for fields quasi-resonant and corotating. This may not be the case since for small g enforcing adiabaticity requires a large Stokes field $\mathcal{W}_s$. In Fig. 2 in the main text we used a peak value of $\mathcal{W}_s$ which would yield e–g Rabi oscillations with angular frequency $\Omega_0 = 600$ MHz). Large fields produce Stark shifts of the detuned transitions: shift of level j due to the coupling to level i under the action of the k field is given by

$$S_{ij}^{(k)}(t) = \left|\frac{\eta_{ij}\mathcal{W}_k(t)}{2}\right|^2\left(\frac{1}{E_i - E_j - \omega_k} + \frac{1}{E_i - E_j + \omega_k}\right)$$

where η_{ij} is the ratio of the dipole matrix element of the selected transition with the reference e–g one. The main effect is due to the term $W_s(t)[|0u\rangle\langle\Phi_0| + |\Phi_0\rangle\langle 0u|]$ and affects the $|0u\rangle - |\Phi_0\rangle$ transition. In the three-level approximation the dynamical Stark shift induces a stray detunings $\delta(t) = -S_{0u,0}^{(s)}(t)$, comparable to Ω_s, which completely suppresses STIRAP[36,49].

Actually the three-level analysis must be generalized to account for the multilevel nature of the system. The relevant stray detuning is $\delta(t) = \sum_{j\neq 2u}S_{2u,j}^{(s)}(t) - \sum_{j\neq 0u}S_{0u,j}^{(s)}(t)$, this structure determining self-compensations which fortunately mitigate the detrimental effect of dynamical Stark shifts. We studied numerically this problem considering up to 40 levels and a control field with the structure $H_C(t) = W(t)[(|u\rangle\langle g| + (1/\eta)|g\rangle\langle e|) + \text{h.c.}]$, which describes the experimentally relevant case of a ladder type "dipole" coupling to the AA, η being the ratio between the corresponding matrix elements (Fig. 2 in the main text).

The full signal can be recovered if appropriately crafted control is used as shown in Fig. 2 in the main text (thin red curve). One option is to use a phase modulation of the Stokes pulse, as explained in[43], designed to compensate the effect of the Stokes field coupled to the $u-g$ transition only. The fact that this is the relevant source of noise is suggested by success of the strategy even when the drive fully couples to the AA Ladder. Another option, namely to add a suitably designed off-resonant tone $W(t) \rightarrow W(t) + \mathcal{W}_s(t)\cos(2\omega_s t)$, will be discussed elsewhere. Of course by increasing the coupling g a large $\mathcal{W}_s$ is not needed any more and no stray detuning is induced. Dynamical Stark shifts can be neglected and naturally disappear for $g \gtrsim 0.4$.

References

1. Haroche, S. & Raimond, J. M. *Exploring the Quantum* (Oxford University press, 2006).
2. Mohseni, M. *et al.* Commercialize quantum technologies in five years. *Nature* **543**, 171 (2017).
3. Reiserer, A. & Rempe, G. Cavity-based quantum networks with single atoms and optical photons. *Rev. Mod. Phys.* **87**, 1379–1418, https://doi.org/10.1103/RevModPhys.87.1379 (2015).
4. Imamoglu, A. *et al.* Quantum information processing using quantum dot spins and cavity qed. *Phys. Rev. Lett.* **83**, 4204–4207, https://doi.org/10.1103/PhysRevLett.83.4204 (1999).
5. Wallraff, A. *et al.* Strong coupling of a single photon to a superconducting qubit using circuit quantum electrodynamics. *Nature* **421**, 162–167, https://doi.org/10.1038/nature02851 (2004).
6. Schoelkopf, R. J. & Girvin, S. M. Wiring up quantum systems. *Nature* **451**, 664 (2008).
7. Plastina, F. & Falci, G. Communicating josephson qubits. *Phys. Rev. B* **67** (2003).
8. Gu, X., Frisk Kockum, A., Miranowicz, A., Liu, Y.-X. & Nori, F. Microwave photonics with superconducting quantum circuits. *Physics Reports* **718–719**, 1–102 (2017).
9. Ciuti, C., Bastard, G. & Carusotto, I. Quantum vacuum properties of the intersubband cavity polariton field. *Phys. Rev. B* **72**, 115303, https://doi.org/10.1103/PhysRevB.72.115303 (2005).
10. Niemczyk, T. *et al.* Circuit quantum electrodynamics in the ultrastrong-coupling regime. *Nature Physics* **6**, 772–776, https://doi.org/10.1038/nphys1730 (2010).
11. Forn-Daz, P. *et al.* Observation of the bloch-siegert shift in a qubit-oscillator system in the ultrastrong coupling regime. *Phys. Rev. Lett.* **105**, 237001, https://doi.org/10.1103/PhysRevLett.105.237001 (2010).
12. Forn-Daz, P. *et al.* Ultrastrong coupling of a single artificial atom to an electromagnetic continuum. *Nat. Phys.* **13**, 39 (2017).
13. Yoshihara, F. *et al.* Superconducting qubit-oscillator circuit beyond the ultrastrong-coupling regime. *Nat. Phys.* **13**, 44 (2017).
14. Bosman, S. *et al.* Multi-mode ultra-strong coupling in circuit quantum electrodynamics. *npj Quant. Inf.* **3**, 46, https://doi.org/10.1038/s41534-017-0046-y (2017).
15. Anappara, A. A. *et al.* Signatures of the ultrastrong light-matter coupling regime. *Phys. Rev. B* **79**, 201303, https://doi.org/10.1103/PhysRevB.79.201303 (2009).
16. Günter, G. *et al.* Sub-cycle switch-on of ultrastrong light–matter interaction. *Nature* **458**, 178–181, https://doi.org/10.1038/nature07838 (2009).
17. Scalari, G. *et al.* Ultrastrong coupling of the cyclotron transition of a 2d electron gas to a thz metamaterial. *Science* **335**, 1323–1326 (2012).
18. Bayer, A. *et al.* Terahertz light–matter interaction beyond unity coupling strengt. *Nano Lett.* **17**, 6340–6344, https://doi.org/10.1021/acs.nanolett.7b03103 (2017).
19. Carusotto, I., De Liberato, S., Gerace, D. & Ciuti, C. Back-reaction effects of quantum vacuum in cavity quantum electrodynamics. *Phys. Rev. A* **85**, 023805, https://doi.org/10.1103/PhysRevA.85.023805 (2012).
20. Stassi, R., Ridolfo, A., Di Stefano, O., Hartmann, M. J. & Savasta, S. Spontaneous conversion from virtual to real photons in the ultrastrong-coupling regime. *Phys. Rev. Lett.* **110**, 243601, https://doi.org/10.1103/PhysRevLett.110.243601 (2013).
21. Di Stefano, O. *et al.* Feynman-diagrams approach to the quantum Rabi model for ultrastrong cavity qed: stimulated emission and reabsorption of virtual particles dressing a physical excitation. *New J. Phys.* **19**, 053010 (2017).
22. Huang, J.-F. & Law, C. K. Photon emission via vacuum-dressed intermediate states under ultrastrong coupling. *Phys. Rev. A* **89**, 033827, https://doi.org/10.1103/PhysRevA.89.033827 (2014).
23. Ridolfo, A., Leib, M., Savasta, S. & Hartmann, M. Photon blockade in the ultrastrong coupling regime. *Phys. Rev. Lett.* **109**, 193602 (2012).
24. De Liberato, S., Ciuti, C. & Carusotto, I. Quantum vacuum radiation spectra from a semiconductor microcavity with a time-modulated vacuum rabi frequency. *Phys. Rev. Lett.* **98**, 103602, https://doi.org/10.1103/PhysRevLett.98.103602 (2007).
25. Bergmann, K., Theuer, H. & Shore, B. Coherent population transfer among quantum states of atoms and molecules. *Rev. Mod. Phys.* **70**, 1003–1025, https://doi.org/10.1103/RevModPhys.70.1003 (1998).
26. Vitanov, N., Fleischhauer, M., Shore, B. & Bergmann, K. Coherent manipulation of atoms and molecules by sequential laser pulses. *Adv. in At. Mol. and Opt. Phys.* **46**, 55–190, https://doi.org/10.1016/S1049-250X(01)80063-X (2001).
27. Vitanov, N. V., Rangelov, A. A., Shore, B. W. & Bergmann, K. Stimulated Raman adiabatic passage in physics, chemistry, and beyond. *Rev. Mod. Phys.* **89**, 015006, https://doi.org/10.1103/RevModPhys.89.015006 (2017).
28. Ashhab, S. & Nori, F. Qubit-oscillator systems in the ultrastrong-coupling regime and their potential for preparing nonclassical states. *Phys. Rev. A* **81**, 042311, https://doi.org/10.1103/PhysRevA.81.042311 (2010).
29. Romero, G., Ballester, D., Wang, Y. M., Scarani, V. & Solano, E. Ultrafast quantum gates in circuit qed. *Phys. Rev. Lett.* **108**, 120501, https://doi.org/10.1103/PhysRevLett.108.120501 (2012).
30. Felicetti, S., Douce, T., Romero, G., Milman, P. & Solano, E. Parity-dependent state engineering and tomography in the ultrastrong coupling regime. *Sci. Rept.* **5**, 11818 (2015).
31. Kyaw, T. H., Herrera-Mart, D. A., Solano, E., Romero, G. & Kwek, L.-C. Creation of quantum error correcting codes in the ultrastrong coupling regime. *Phys. Rev. B* **91**, 064503, https://doi.org/10.1103/PhysRevB.91.064503 (2015).
32. Andersen, C. & Blais, A. Ultrastrong coupling dynamics with a transmon qubit. *New J. Phys.* **19**, 023022 (2017).
33. Ashhab, S. Superradiance transition in a system with a single qubit and a single oscillator. *Phys. Rev. A* **87**, 013826 (2013).
34. Jaako, T., Xiang, Z.-L., Garcia-Ripoll, J. J. & Rabl, P. Ultrastrong-coupling phenomena beyond the dicke model. *Phys. Rev. A* **94**, 033850, https://doi.org/10.1103/PhysRevA.94.033850 (2016).
35. Cirio, M., De Liberato, S., Lambert, N. & Nori, F. Ground State Electroluminescence. *Phys. Rev. Lett* **116**, 113601, https://doi.org/10.1103/PhysRevLett.116.113601 (2016).
36. Falci, G. *et al.* Advances in quantum control of three-level superconducting circuit architectures. *Fort. Phys.* **65**, 1600077, https://doi.org/10.1002/prop.201600077 (2017).
37. Siewert, J., Brandes, T. & Falci, G. Adiabatic passage with superconducting nanocircuits. *Opt Commun* **264**, 435–440, https://doi.org/10.1016/j.optcom.2005.12.083, Quantum Control of Light and Matter. In honor of the 70th birthday of Bruce Shore (2006).
38. Wei, L. F., Johansson, J. R., Cen, L. X., Ashhab, S. & Nori, F. Controllable coherent population transfers in superconducting qubits for quantum computing. *Phys. Rev. Lett.* **100**, 113601, https://doi.org/10.1103/PhysRevLett.100.113601 (2008).
39. Siewert, J., Brandes, T. & Falci, G. Advanced control with a cooper-pair box: Stimulated Raman adiabatic passage and fock-state generation in a nanomechanical resonator. *Phys. Rev. B* **79**, 024504, https://doi.org/10.1103/PhysRevB.79.024504 (2009).

40. Kumar, K., Vepsäläinen, A., Danilin, S. & Paraoanu, G. Stimulated Raman adiabatic passage in a three-level superconducting circuit. *Nat. Comm.* **7**, 10628, https://doi.org/10.1038/ncomms10628 (2016).
41. Xu, H. *et al.* Coherent population transfer between uncoupled or weakly coupled states in ladder-type superconducting qutrits. *Nature Communications* **7**, 11018, https://doi.org/10.1038/ncomms11018 (2016).
42. Vepsäläinen, A., Danilin, S., Paladino, E., Falci, G. & Paraoanu, G. S. Quantum control in qutrit systems using hybrid rabi-stirap pulses. *Photonics* **3**, 62, https://doi.org/10.3390/photonics3040062 (2016).
43. Di Stefano, P. G., Paladino, E., Pope, T. J. & Falci, G. Coherent manipulation of noise-protected superconducting artificial atoms in the lambda scheme. *Phys. Rev. A* **93**, 051801, https://doi.org/10.1103/PhysRevA.93.051801 (2016).
44. Rigetti, C. *et al.* Superconducting qubit in a waveguide cavity with a coherence time approaching 0.1 ms. *Phys. Rev. B* **86**, 100506, https://doi.org/10.1103/PhysRevB.86.100506 (2012).
45. Paladino, E., Galperin, Y., Falci, G. & Altshuler, B. 1/f noise: implications for solid-state quantum information. *Rev. Mod. Phys.* **86**, 361–418, https://doi.org/10.1103/RevModPhys.86.361 (2014).
46. Paladino, E., Faoro, L. & Falci, G. Decoherence due to discrete noise in josephson qubits. In Kramer, B. (ed.) *Adv. in Sol. State Phys.*, vol. 43, 747–762 (2003).
47. Peterer, M. J. *et al.* Coherence and decay of higher energy levels of a superconducting transmon qubit. *Phys. Rev. Lett.* **114**, 010501, https://doi.org/10.1103/PhysRevLett.114.010501 (2015).
48. Falci, G. *et al.* Design of a lambda system for population transfer in superconducting nanocircuits. *Phys. Rev. B* **87**, 214515–1,214515–13, https://doi.org/10.1103/PhysRevB.87.214515 (2013).
49. Ridolfo, A., Falci, G., Pellegrino, F. & Paladino, E. Photon pair production by STIRAP in ultrastrongly coupled matter-radiation systems. *Eur. Phys. J. Special Topics* **227**, 183–2188 (2019).
50. Garca-Ripoll, J. J., Peropadre, B. & De Liberato, S. Light-matter decoupling and A^2 term detection in superconducting circuits. *Sci. Rept.* **5**, 16055 (2015).
51. Di Stefano, P. G., Paladino, E., D'Arrigo, A. & Falci, G. Population transfer in a lambda system induced by detunings. *Phys. Rev. B* **91**, 224506, https://doi.org/10.1103/PhysRevB.91.224506 (2015).

Acknowledgements

Author Contributions

G.F. and E.P. conceived the model; A.R. carried out the numerical calculations; G.F. carried out the analytical calculations; G.F., A.R. and G.P.D. analyzed the data. All authors discussed the physics and contributed to writing the manuscript.

Additional Information

Competing Interests: The authors declare no competing interests.

Publisher's note: Springer Nature remains neutral with regard to jurisdictional claims in published maps and institutional affiliations.